Potential of graphene-based materials to combat COVID-19: properties, perspectives, and prospects

A.K. Srivastava[**], N. Dwivedi[*], C. Dhand, R. Khan, N. Sathish, M.K. Gupta, R. Kumar, S. Kumar

CSIR-Advanced Materials and Processes Research Institute, Bhopal, 462026, India

A B S T R A C T

Severe acute respiratory syndrome coronavirus 2 (SARS-CoV-2), a new virus in the coronavirus family that causes coronavirus disease (COVID-19), emerges as a big threat to the human race. To date, there is no medicine and vaccine available for COVID-19 treatment. While the development of medicines and vaccines are essentially and urgently required, what is also extremely important is the repurposing of smart materials to design effective systems for combating COVID-19. Graphene and graphene-related materials (GRMs) exhibit extraordinary physicochemical, electrical, optical, antiviral, antimicrobial, and other fascinating properties that warrant them as potential candidates for designing and development of high-performance components and devices required for COVID-19 pandemic and other futuristic calamities. In this article, we discuss the potential of graphene and GRMs for healthcare applications and how they may contribute to fighting against COVID-19.

© 2020 Elsevier Ltd. All rights reserved.

1. Introduction

The recent outburst of coronavirus disease-19 (COVID-19) is devastating for global health systems [1,2]. COVID-19 is a fatal disease that is caused by a newly born severe acute respiratory syndrome coronavirus 2 (SARS-CoV-2) [1,2]. Due to its severity and reach to most of the nations across the world, the world health organization (WHO) has declared it a pandemic [1,2]. As of June 11, 2020, there are more than 7.597 million confirmed cases with about 3.841 million recoveries and about 0.423 million deaths for COVID-19 affecting 215 countries [3]. To date, there is no medicine or vaccine available for COVID-19 treatment, though the research, development, and clinical trials for both medicines and vaccines are under progress at an unbelievable pace.

Over the past few years, graphene and graphene-related materials (GRMs) have attracted huge attention of the researchers owing to their wide spectrum properties such as high surface area, high electrical mobility and conductivity, excellent mechanical, electrochemical, and piezoelectric properties, and efficacy against

microbes and viruses [4–14]. Recently, few good reviews appeared in the literature revealing the authors' views and projections on the possible contribution of graphene-based materials in the global fight against COVID-19 [15–17]. For example, Palmeri and Papi [15] have emphasized over the various modes of interactions among graphene materials and different virions that can help in blocking or destroying the viruses. The authors also briefed over the plausible role of the graphene textiles and filters in controlling the epidemiological spread of COVID-19 and the implications of graphene materials for the development of environmental sensors. Udugama et al. [16] focused on discussing the emerging diagnosis technologies for COVID-19 detection. These technologies include reverse transcription recombinase polymerase amplification (RT-RPA), loop-mediated isothermal amplification method (LAMP), nucleic acid sequence-based amplification (NASBA), rolling circle amplification, enzyme-linked immunosorbent assay (ELISA), magnetic biosensor, magnetic ELISA, and DNA-assisted immunoassay, which all mainly used nucleic acid and protein biomarkers for viral and bacterial diagnosis [16]. Cordaro et al. [17] compiled the literature on the contribution of graphene-based materials and strategies in liquid biopsy and the diagnosis of viral diseases and discussed the potential of graphene in COVID-19 diagnosis. In general, most of the recent reports briefly reviewed the literature related to the implications of graphene-related materials in virus diagnosis and their role in designing personal protective

---

* Corresponding author.
** Corresponding author.
   E-mail addresses: director@ampri.res.in (A.K. Srivastava), neeraj.dwivedi@ampri.res.in, neerajdwivedi6@gmail.com (N. Dwivedi).

equipment with special reference to COVID-19. In the present re-view, we have discussed in detail the various functional properties of graphene and related materials and their plausible role in the global fight against viral diseases including COVID-19 by designing highly sensitive electrochemical, piezoelectric, field-effect transistor-based biosensors, and surface plasmon resonance-based diagnostic systems. The article further covers the importance of graphene oxide and related materials in controlling the virus spread and transmission including COVID-19 due to their potential role in (i) development of antiviral surfaces/coatings, (ii) designing of nanofoams for face masks and other PPEs, and (iii) fabrication of 3D printed medical components. Fig. 1 illustrates different possible applications of graphene and GRMs to combat different problems related to viral infections including COVID-19 spread.

Their potency to destabilize and kill microbes and viruses could lead to the application of graphene and GRMs, especially metal ions decorated GRMs, in the development of antiviral and antimicrobial materials and surfaces that may be used in hospital settings, high touch surfaces, and various consumer products. The excellent electrical, electrochemical, piezoelectric properties may enable their applications in the development of electrochemical bio-sensors, field-effect transistor (FET)-based biosensors, and piezo-electric biosensors for rapid, cost-effective, sensitive, and early-stage diagnosis of viruses. Graphene and GRM-based materials could be used as surface plasmon resonance (SPR) substrate to design highly sensitive viral diagnostic devices, their nanofoams could be used in the development of highly effective face masks with controlled porosity on nanoscale, and 3D printing of these materials may lead to design and development of a variety of PPEs

and other healthcare components. We discussed in detail the possible technology development based on graphene and GRMs to fight against COVID-19 and other futuristic health calamities.

2. Graphene and graphene-related materials

Graphene is an atomically thin layer (single layer) of sp^2 bonded carbon atoms arranged in a hexagonal pattern (Fig. 2a). Single-layer graphene (SLG) displays outstanding properties. In SLG, the π and π^* bands touch at the Dirac point that makes it a zero-band gap material, and at Dirac point, the SLG electrons behave-like massless fermions (Fig. 2b) [4−7]. SLG displays high carrier mobility that can reach to about $10^5–10^6$ cm^{2}V^{-1}s^{-1}, two to three orders of magnitude higher than silicon; high mechanical strength of about 130 GPa (130 GPa = 13256310768.713 kg/m^2), several times higher than steel; electrical and thermal conductivities higher than copper and diamond, respectively; high transmission of about 97.7%; excellent lubricity; broad-spectrum antimicrobial properties, etc. [4−14]. Graphene and GRMs can be produced by various top-down and bottom-up approaches [4−7]. Dry and liquid exfoliations are among the common methods for the synthesis of graphene. Geim and Novoselov used the mechanical exfoliation method to peel off the graphite through the scotch tape to produce graphene [4]. Thermal chemical vapor deposition (CVD) is one of the best methods for the synthesis of high-quality graphene with minimal defects [5] that could be used in the development of graphene field-effect transistor (FET), electrochemical, and piezoelectric bio-sensors. The CVD process of graphene production requires the thermal decomposition of carbon-containing precursor gas, mainly
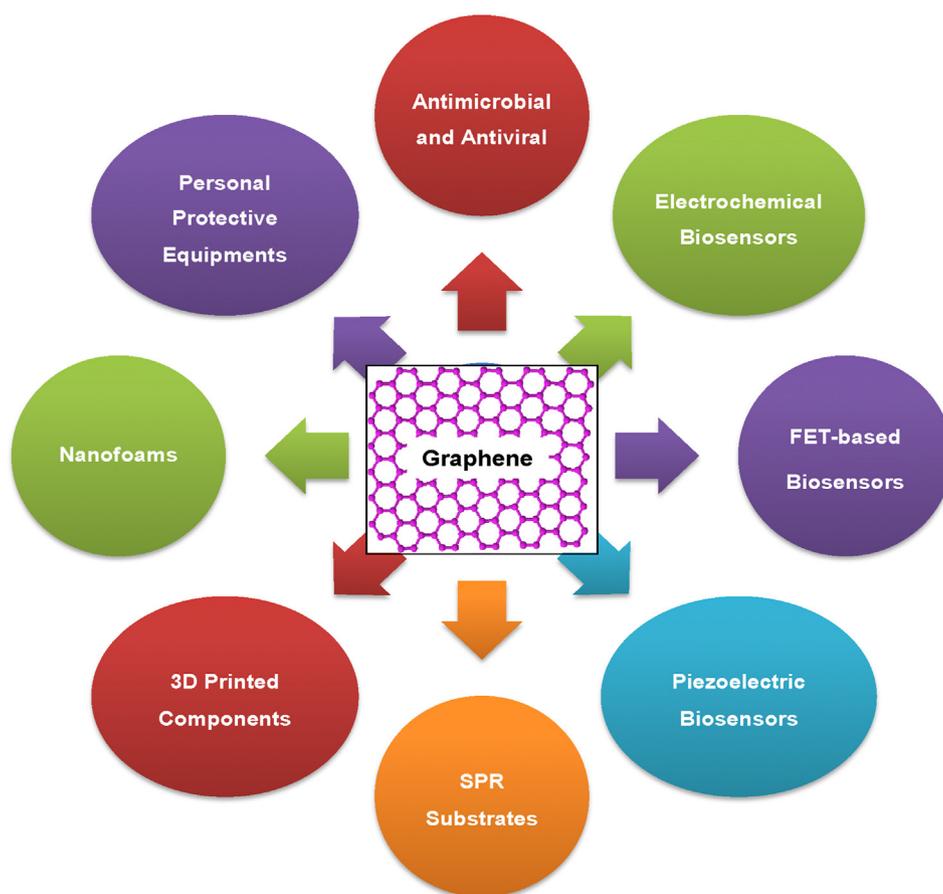

Fig. 1. Graphene and GRMs could be explored for the development of a number of components and devices that are essentially required to combat infectious diseases including COVID-19.
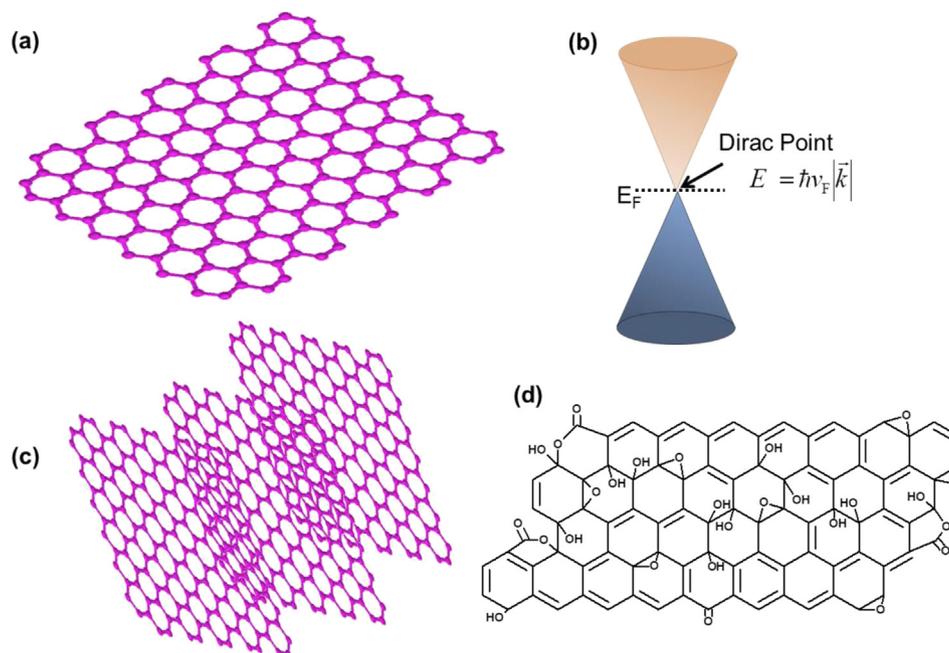
Fig. 2. Schematic illustration of the graphene and GRMs. (a) Single-layer graphene, (b) energy-momentum diagram for one of the discrete points of graphene's Brillouin zone showing conduction and valence bands touching at the Dirac point, (c) multilayer graphene, and (d) graphene oxide.

methane, at a high temperature of about 1000 °C on a specific substrate viz. copper [18]. Other materials such as Ni [19], Pt [20], Fe [21], and their alloys [22] have also been employed as the substrates for the deposition of the graphene layer. Preconditioning of the substrate is also required before the deposition of high-quality graphene on copper [22]. Once the synthesis of graphene has been done on a specific substrate, the transfer methods are employed to place the graphene on desired surfaces. Commonly, the transfer of graphene from Cu foil to the desired substrate requires the following steps: (i) coating of poly(methyl methacrylate) (PMMA) on graphene on copper, where PMMA acts as a support layer for graphene, (ii) etching of copper in FeCl$_3$ solution, (iii) rinsing of PMMA/graphene film with ultrapure water, (iv) lifting off PMMA/graphene film on a desired substrate, (v) removal of PMMA, and cleaning and baking of the graphene to get good quality transferred graphene [23]. Likewise, GRMs, such as bilayer graphene (BLG) and multilayer graphene (Fig. 2c), can be obtained by repeated transfer of the SLG on top of one another. Unlike SLG, the BLG has a greater feasibility to tune its bandgap and hence in recent past this material has attracted considerable interest for optoelectronic applications in particular. The engineering of the bandgap and other properties of BLG and MLG can be performed by the application of electric field, and chemical doping [4–7]. The top-down approach is the simple, scalable, and fast method for the synthesis of GRMs such as graphene oxide (Fig. 2d), which is an oxide sheet of graphene. Hummer's, Brodie, and Staudenmaier methods or modified versions of these methods are used for the synthesis of GO [24]. Graphite is the starting material that is oxidized in an acidic environment, and then ultrasonication and purification steps are employed to reduce the number of layers of graphite oxide to a few layer GO, and even single-layer GO. Furthermore, GO possesses a bandgap due to the presence of functional groups but it shows inferior electrical and thermal properties than graphene [4–7]. It is essential for many applications, in particular for electronics and bio-electronics like biosensors, to enhance the conductivity of GO to develop highly sensitive, selective, and fast sensing devices. Thus, the chemical reduction of GO is performed commonly using

hydrazine, and the resultant reduced graphene oxide (rGO) demonstrates considerably improved electrical properties than GO [4–7]. This is attributed to a reduced amount of oxygen-containing groups in rGO with respect to GO, but the electrical properties of rGO remain slightly inferior to pristine graphene [4–7]. A detailed description of the synthesis and properties of graphene and GRMs can be found in Ref. [5,7,24,25].

3. Graphene-based anti-viral surfaces and coatings

Unveiled in December 2019, a new fatal SAR-CoV-2 virus starts circulating among humans [26]. Transmission through sub-micron size respiratory droplets is the common pathway for COVID-19 spread [27]. Moreover, a person can also catch this virus by coming in contact with the contaminated objects or surfaces and then touching their mouth, nose, or eyes. A recent study reported the variable stability of the SAR-CoV-2 virus on different surfaces [28]. The SARS-CoV-2 is found to have a higher survival time on plastic (72 h) and stainless steel (48 h) surfaces compared to copper (4 h) and cardboard (24 h). Moreover, the virus is confirmed to be more stable on smooth surfaces compared to rough surfaces such as printing/tissue papers (3 h), wood (2 h), and cloths (2 h). Unfortunately, the detectable level of the virus is reported to be available on the external layer of the surgical masks even on day 7 [29]. Thus, contaminated high touch surfaces that offer high virus stability can enhance the chances of COVID-19 spread. In the present pandemic situation, where the COVID-19 cases are exponentially increasing each day globally, the development of efficient anti-SARS-CoV-2 protective surfaces/coatings can play a significant role in controlling the viral spread through high touch components, products, and systems.

Graphene-based materials have been explored extensively for their antimicrobial potentials [14,30]. Reported studies provided evidence about the broad-spectrum inhibition activity of graphene oxide and its derivatives against bacteria [31] and fungi [32]. In 2014, Sametband et al. [33] reported the antiviral properties of GO and partially reduced sulfonated GO against Herpes Simplex Virus Type-

1 (HSV-1) through competitive inhibition mechanism. Similar to cell surface receptor heparan sulfate, GO and rGO-SO₃ contain multiple negatively charged groups and thus both moieties compete with each other in binding with HSV-1. Blocking of the virus binding sites with the nanomaterial was the main inhibitory factor to safeguard Vero cells from infection. Ye et al. [34] have compared the antiviral potency of GO, rGO, GO-polyvinylpyrrolidone (PVP) composite, GO-poly(diallyldimethylammonium chloride) (PDDA) composite with precursors graphite (Gt), and graphite oxide (GtO). The study revealed broad-spectrum antiviral activity of GO against Pseudorabies virus (PRV, a DNA virus) and porcine epidemic diarrhea virus (PEDV, an RNA virus). Results also suggest that the antiviral properties of GO are attributed to its negatively charged, sharp-edged structure. The GO conjugated with polyvinylpyrrolidone (PVP, non-ionic polymer) showed potent antiviral activity; however, PDDA (cationic polymer) bound GO revealed no virus inhibition, suggesting negative charge as a prerequisite for antiviral properties.

Song et al. [35] have reported the GO-based label-free method to detect and disinfect environmental viruses such as Enterovirus 71 (EV71) and endemic gastrointestinal avian influenza A virus (H9N2) that have great environmental stability and low sensitivity for organic disinfectants and soaps. The report suggests that the physicochemical interactions (hydrogen bonding, electrostatic, redox reactions) among GO and viruses, under thermal reduction of GO, play a critical role in capturing and destruction of the viruses. The viricidal properties of GO are found to be enhanced under elevated temperature conditions (56 °C). In another report, GO sheets are reported to exhibit significant antiviral inhibition potentials toward enveloped feline coronavirus (FCoV), and incorporating silver particles into GO structure broadens its antiviral potential toward non-enveloped infectious bursal disease virus (IBDV) as well [36]. Yang et al. [37] have prepared multifunctional curcumin loaded β-CD functionalized sulfonated graphene composite (GSCC) and investigated its antiviral potential against negative sense respiratory syncytial virus (RSV) which like SARS-CoV-2 infects both the lower and upper respiratory tracts with children and elderly as their easy targets. The results revealed that GSCC could inhibit RSV from infecting the host cells by inactivating the virus directly and prohibiting the attachment of the virus and have prophylactic and therapeutic effects toward the virus. In a recent study, authors have attempted to investigate the antiviral effect of GO-Silver nanoparticles composite on the replication of porcine reproductive and respiratory syndrome virus (PRRSV) [38]. The results suggest that the exposure of virus with GO-AgNPs composite obstruct the virus to enter the host cell with 59.2% efficiency and also promotes the production of IFN-stimulating genes (ISGs) and interferon-α (IFN-α) that inhibits the virus proliferation. Table 1 shows the application of various graphene oxide derivatives for antiviral properties with their mechanisms of action.

In general, GO and its derivatives have wide-spectrum antiviral properties such as against positive sense and negative sense viruses, RNA and DNA viruses, and enveloped and non-enveloped viruses. Thus, these materials have immense potential in the development of antiviral surfaces and coatings for preventing contamination from virulent and contagious viruses including SARS-CoV-2 and could control the disease transmission. Particularly, for the SAR-CoV-2 virus, considering the virus structure rich in −COOH functionalities and lower survival time of this virus on copper surfaces, GO/rGO-SO₃ coatings enriched with copper nanoparticles/copper ions could be promising candidates for the development of anti-SARS-CoV-2 surfaces. The composite structures of GO/rGO-SO₃ with antimicrobial metals including silver, titanium, and gold could also be explored to unveil their potential in the fabrication of effective antiviral coating designs. These

materials can help in effectively capturing and destabilizing the virus structures and minimize their survival time on diverse coated surfaces. Fig. 3 shows how the coatings of graphene, GRMs or graphene/GRMs-metal ions composite may limit the lifetime of the viruses on diverse high touch surfaces.

4. Graphene-based electrochemical biosensors

Early-stage, accurate, and rapid detection of viruses is a prerequisite to control the infection spread. In particular, the commonly available diagnostic kits for the diagnosis of the SARS-CoV-2 virus are based on polymerase chain reaction (PCR) such as RT-PCR [39]. While the RT-PCR-based technique is highly sensitive and shows significant specificity for SARS-CoV-2, it is a slow diagnostic method (3−4 h) and has a high cost. Thus, the development of a rapid, economical viable, and reliable point-of-care (POC) test for detection of SARS-CoV-2 viral infection is the need of the hour. Biosensors are potential candidates for the detection of biomolecules and viruses. The surface of the biosensor is important in the performance of the analytical device; it is where immobilization and transduction take place [40]. Researchers have developed electrochemical-, colorimetric-, lateral flow-, SERS-based biosensors, etc., which have the advantages of high sensitivity and selectivity, cost-effectiveness, portability, and easy to use. The gold and carbon electrodes have been used as electrochemical transducers for fast and sensitive biosensors [41]. Refs [42,43] show the development of an impedance-based boron-doped diamond biosensor for early detection of the influenza M1 virus. Electrochemical biosensors in particular are considered as reliable and sensitive biosensors [39,44]. Nanomaterials [45] are often used to amplify the signal and sensitivity of electrochemical biosensors. In electrochemical biosensors, any electrochemical change at the interface between electrodes and an electrolyte, based on a conformational change produced by biometric recognition between antibody and antigen, is measured.

Graphene has been explored to design highly efficient biosensors due to its stable electrochemical and optical behavior, high electrocatalytic activity, and excellent mechanical and thermal properties [46]. Graphene-based platforms have been used to immobilize biomolecules to create biosensors. Ref. [47] describes the method to immobilize the biomolecules onto the graphene surface via surface chemical engineering. These strategies include covalent bonding, such as the coupling of the biomolecules via 1-ethyl-3-(3-dimethylamino propyl) carbodiimide hydrochloride and N-hydroxysuccinimide reactions, and physisorption. Detection of the Zika virus by graphene-enabled portable biosensor was demonstrated by Afsahi et al. [48]. Likewise, Joshi et al. (2019) [49] reported the detection of the influenza virus using graphene oxide-based biosensor. The detection limit for the target virus was measured to be 26 and 33 PFU/mL in PBS and saliva samples, respectively. Huang et al. [50] reported highly sensitive electrochemical biosensor based on chitosan/Silver nanoparticle (AgNPs)-graphene composite materials. The developed biosensor shows efficacy in detecting the avian influenza virus H7 (AIV H7) with a detection limit as low as 1.6 pg/mL. Thus, the effectiveness of graphene-based electrochemical biosensors for the detection of biomolecules, in particular for the viruses, suggests that these biosensors have the potential to effectively detect the novel coronavirus SARS-CoV-2 as well [51] but a lot of high-end research needs to be performed to develop reliable diagnostic devices. We present a hypothetical mechanism in Fig. 4 that shows how electrochemical biosensors based on graphene and GRMs could be used for the detection of the SARS-CoV-2 virus. Table 2 shows the literature on graphene and GRMs-based electrochemical biosensors for the detection of various viruses.

Table 1
Antiviral property of GO and its derivatives against different types of viral strains.

Graphene Derivative	Virus Targeted	Inhibition Mode/Mechanism	Important Findings	References
GO and rGO-SO3	**HSV-1** (DNA virus, infecting 70—90% human population, mostly target epithelial cells and neuron of PNS, leads to oral lesions, ocular diseases and encephalitis in rare cases)	Competitive Inhibition Mechanism	Both graphene derivatives inhibit the virus at low concentrations (ng/mL) which leads to a reduction in plaque formation. Cytotoxicity experiments showed the non-toxic nature of graphene nanomaterials.	[33]
GO, rGO, Gt, GtO, GO-PVP, GO-PDDA	**PRV** (DNA virus, infect most of the mammals, cause lesions primarily in CNS, respiratory system and reproductive system) **PEDV** (RNA virus, belonging to positively charged alpha-coronavirus, responsible for high mortality rate in Pigs)	The antiviral mechanism is attributed to the negative charge of GO and its nanosheet structure.	GO inactivated both viruses (PRV, PEDV) by structural destruction prior to the viral entry into the cell. But it does not inhibit after the onset of viral infection. GO exhibits antiviral properties even at a low non-cytotoxic concentration (1.5 μg/mL). Cationic GO-PDDA has no antiviral activity, however, non-ionic GO-PVP shows antiviral activity similar to GO, which suggests that the negative charge is required for the antiviral properties. Polylaminate GtO revealed a much weaker inhibitory effect than single-layered GO and rGO, whereas Gt having non-nanosheet structure shows no antiviral activity, suggesting that the nanosheet structure is vital for the antiviral activity.	[34]
GO	**EV71** (RNA capsid Virus, Capsid Virus, Responsible for hand, foot, and mouth disease, very common among children) **H9N2** (RNA enveloped virus, causes human influenza as well as bird flu)	The GO-Virus physiochemical interactions lead to virus capturing and RNA leakage from the virus.	GO significantly supports absolute destruction, exclusion, and dis-infection features to attain a minimum 6-log loss of infectivity. Disinfectant effect of the GO against virus is found to be enhanced under elevated temperature and prolonged exposure time.	[35]
GO and GO-Ag particles	**FCoV** (positive-sense, enveloped RNA virus with lipid envelope, leads to feline infectious peritonitis which is a growing fatal disease in cats) **IBDV** (non-enveloped RNA virus, infect chicken and leads to immunosuppression)	Chemical interactions among the GO/GO-Ag structure including electrostatic interactions, Vander walls interactions, and Ag—SH binding leads to virus destructions.	Integration of Ag particles in GO sheets enhances the viricidal properties of GO toward enveloped viruses and also broadens its inhibitory effect to non-enveloped viruses also.	[36]
Curcumin-loaded β-CD functionalized sulfonated graphene	**RSV** (enveloped RNA virus, 150 nm in diameter, can infect the upper and lower respiratory tract, commonly cause respiratory illness in newly born infants, children, elderly, and immunocompromised individuals)	Three proposed mechanisms are GSCC inhibiting RSV infection by inactivating RSV directly, inhibition of the attachment of virus with host cells, and interference in virus replication.	The effective concentration of GSCC is found to be non-toxic to the host cells. The viral titer showed four orders of reduction using GSCC.	[37]
GO-AgNPs	**PRRSV** (single-stranded positive-sense RNA virus, mostly infect the pigs)	Inhibitory role is due to posing a hindrance to the virus to enter the host cell and by promoting the generation of ISGs and IFN-α.	Plaque assays indicated that GO-AgNPs nanocomposites have an inhibitory effect on the virus in entering the host cells thereby suppressing virus replication.	[38]

Abbreviations: GO-Graphene Oxide; **rGO-SO₃**- reduced sulfonated graphene oxide; **HSV-1**- Herpes Simplex Virus Type-1; **rGO**- reduced graphene oxide; **Gt**- Graphite; **GtO**- Graphite Oxide; **PVP**- Polyvinylpyrrolidone; **PDDA**-poly (diallyl dimethylammonium chloride); **PRV**- Pseudorabies virus; **PEDV**- porcine epidemic diarrhea virus; **EV-71**- Enterovirus-71; **H9N2**- endemic gastrointestinal avian influenza A virus; **FCoV**- feline coronavirus; **IBDV**- infectious bursal disease virus; **β-CD**- β Cyclodextrin; **RSV** - respiratory syncytial virus; **GSCC** — Curcumin loaded β-CD functionalized sulfonated graphene; **AgNPs** — Silver Nanoparticles; **PRRSV**- porcine reproductive and respiratory syndrome virus.

5. Graphene-based field-effect transistor for biosensing

Graphene field-effect transistors (GFET) have huge potential for sensitive, fast, and early detection of viruses; many recent works indeed show its application for virus detection. GFET employs an ultrathin graphene channel between the source and the drain. Chen et al. [52] demonstrated the application of GFET for the detection of Ebola virus antigen. The rGO was placed between the electrodes to form the sensitive and conducting channel and alumina was coated on the rGO for surface passivation [52]. The Ebola antibodies were conjugated with gold nanoparticles on rGO channel and acted as a sensing platform. The developed GFET displayed high sensitivity with a limit of detection down to 1 ng/mL for Ebola glycoprotein (EGP) [52]. Ono et al. [53] demonstrated the detection of the influenza virus using GFET; the GFET device was prepared using the exfoliated graphene on Si/SiO2 substrate having metal electrodes. Ref. [54] demonstrates the application of liquid coplanar gate GFET made on a flexible polyethylene terephthalate substrate for the detection of the human immunodeficiency virus (HIV-1) and murine leukemia virus (MLV). The GFET device revealed attomolar (aM) level detection of viruses with a detection limit approaching 48.7 aM that makes GFET a highly sensitive device for virus detection. Jin et al. [55] showed the use of rGO-based FET for the detection of the Ebola virus with a detection limit of the device as low as 2.4 pg/mL.
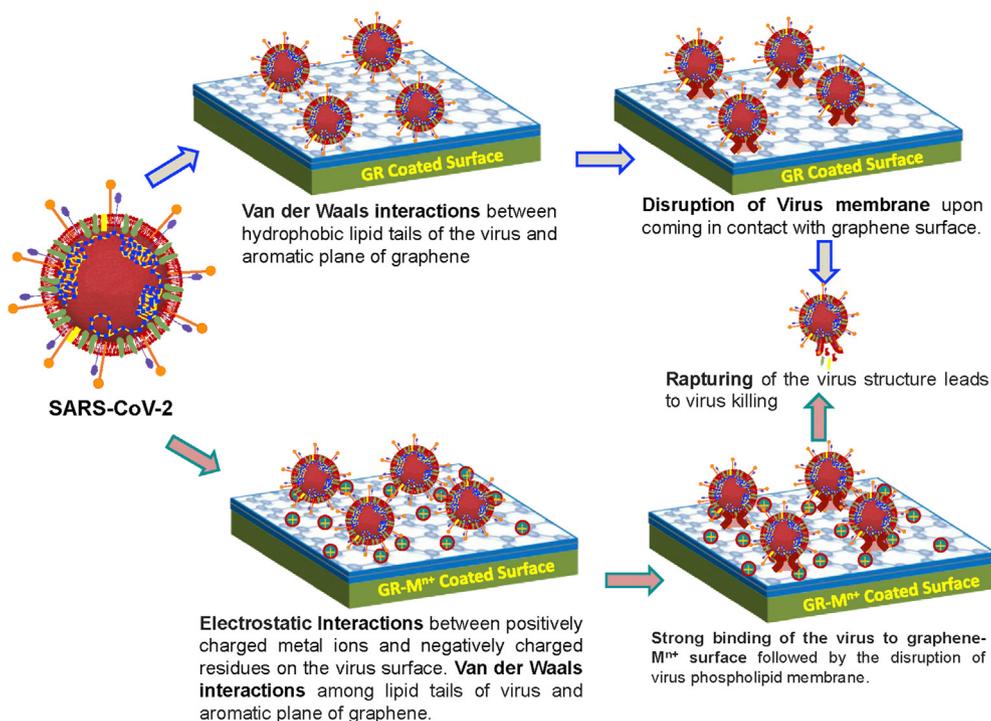
Fig. 3. Schematic reveals the possible role of graphene (GR) and GR-metal ion-coated surfaces in inhibiting surface contamination from viruses including SARS-CoV-2.

Likewise, Pant et al. [56] demonstrated the application of rGO-based FET for the detection of rotavirus. These findings suggest that GFET-based sensing platforms could be utilized for sensitive and fast detection of SARS-CoV-2. The prediction of GFET as a sensing device for SARS-CoV-2 has recently been turned into a reality as Seo et al. [57] successfully demonstrated the detection of SARS-CoV-2 in human nasopharyngeal swab specimens using GFET. The GFET biosensor was created by applying a specific antibody, which acts against SARS-CoV-2 spike protein, on the graphene channel. The developed GFET sensor demonstrated extraordinary sensing properties in terms of its high sensitivity for the detection of SARS-CoV-2 spike protein at concentrations of 100 fg/mL in clinical transport medium, and 1 fg/ML in phosphate-buffered saline. Moreover, GFET successfully detected the SARS-CoV-2 in cultured medium and clinical samples were taken from COVID-19 patients [57]. This discovery is extremely important to speed up the detection of SARS-CoV-2 among humans as the present reliable diagnostic tool viz. RTPCR is expensive and time consuming that renders diagnostic of the large human population; escalating the COVID-19 testing is the need of the hour. While the initial results are promising, a significant amount of work is yet to be performed to fully understand the GFET for designing sensitive and fast biosensor devices for the accurate detection of SARS-CoV-2. Table 2 compiles the literature on graphene and GRMs-based FET biosensors for the detection of various viruses including SARS-CoV-2.
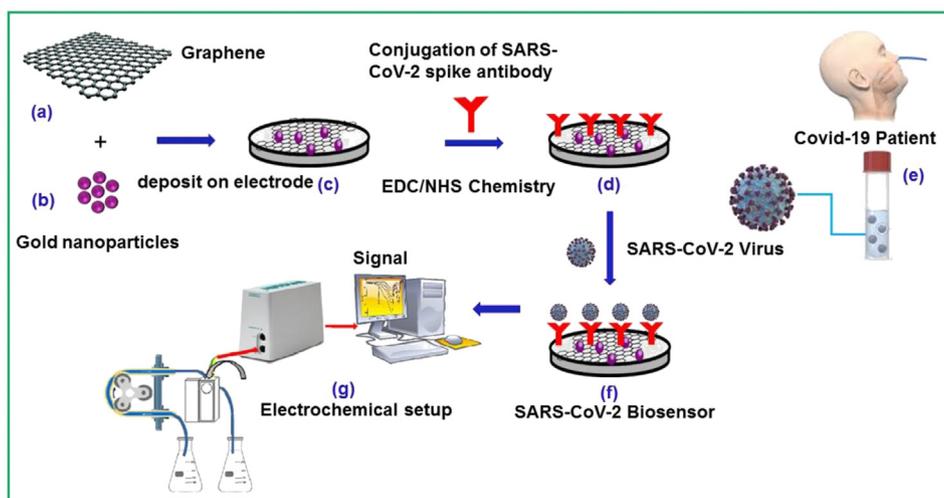

Fig. 4. Methodology to design affinity electrochemical biosensors for the detection of SARS-CoV-2 virus. Materials selection (a) graphene and (b) gold nanoparticles, (c) their deposition on electrode material, (d) conjugation of SARS-CoV-2 spike antibody on decorated electrode, (e) sample of COVID-19 patient, (f) SARS-CoV-2 biosensor, and (g) electrochemical set up for detection.

Table 2
The overview of so far reported electrochemical biosensor works dealing with various virus detection on graphene and composites-based materials.

Materials	Sensor Type/Method	Sensing Performance (Sensitivity/Detection limit)	Others (Biomarker)	Ref.
Array of gold nanoparticle-modified carbon electrodes	Square wave voltammetry (SWV)	0.4 and 1.0 pg mL^{-1}	Proteins such as Influenza	[43]
Reduced graphene oxide	Electrochemical Impedance Spectroscopy	26 and 33 plaque-forming units	Plaque	[49]
Gold nanoparticle-graphene nanocomposites	Amperometric	1.6 pg/mL	Monoclonal antibodies (MAbs)	[50]
Graphene-gold hybrid nanocomposite	Amperometric	10-8 U mL^{-1} N	PNA lectin	[72]
Reduced graphene oxide	Electrochemical	0.5 PFU mL^{-1}	Monoclonal antibodies	[73]
Graphene oxide surface by APTES	Impedimetric	1 fM	DNA target	[74]
Silver nanoparticles/graphene quantum dots	Electrochemical	3 fg mL^{-1}	Antibody	[75]
Graphene oxide	Electrochemical	8.3 fM	Immunodeficiency Virus Type 1 (HIV-1)	[76]
Functionalized graphene with amino groups	Electrochemical	0.1 ng mL-1	Antibodies (anti-p2)	[45]
Fluorinated tin oxide/gold nanoparticle sensor	Electrochemical	90 fM	Monoclonal antibody (nCovid-19Ab)	[77]
Reduced graphene oxide	Field-effect transistor	Detection limit down to down to 1 ng/mL	Ebola glycoprotein	[52]
Graphene	Field-effect transistor	–	Human-type 2.6 sialoglycan (for influenza virus)	[53]
Graphene	Field-effect transistor	47.8 aM-10.5 nM	HIV-1 and MLV).	[54]
Reduced graphene oxide	Field-effect transistor	Detection limit as low as 2.4 pg/mL	Ebola virus glycoprotein (for Ebola virus detection)	[55]
Reduced graphene oxide	Field-effect transistor	101 to 106 particle/mL.	Rotavirus antigen (for rotavirus detection)	[56]
Graphene	Field-effect transistor	Detection at concentrations of 1 fg/mL in PBS and 100 fg/LmL clinical transport medium	SARS-Cov-2 spike protein (for SARS-Cov-2 detection)	[57]
BSA precoated Crystal	Piezoelectric microbalance	50 pg L^{-1}	protein antigen/IgG antibody	[58]
Graphene interdigitated gold electrode piezoelectric sensors	Piezoelectric Quartz Crystal microbalance	41 cfu/mL	*Staphylococcus aureus*	[78]
Piezoelectric Crystal	Piezoelectric immunosensor	0.6–4 µg/mL	SARS-associated coronavirus (SARS-CoV	[65]
Au surfaces on piezoelectric quartz	Piezoelectric Sensors	0.8–38.8 mM	Hepatitis B virus (HBV)	[66]
Oligonucleotide functionalized gold nanoparticles on piezoelectric crystal	Quartz Crystal Microbalance	2–2 10^6 PFU/mL	Dengue virus	[79]
Gold nanoparticles (AuNPs) on piezoelectric Quartz Crystal microbalance	(QCM) piezoelectric immunosensor	0–1 log CFU/mL	Viable bacterial cells	[68]

6. Graphene-based piezoelectric biosensors

Piezoelectric biosensors have become a popular technology to detect viruses, hormones, bacteria, cells and to study a broad range of biomolecular interactions. Piezoelectric biosensor offers real-time and label-free transduction with high sensitivity, simplicity, and swiftness [58–61]. Particularly, the piezoelectric immunosensor was first developed by Shons in 1972 to detect cow serum IgG antibody [58]. Among them, piezoelectric quartz crystal microbalance biosensor has become important to detect various coronaviruses that work on the principle of piezoelectricity, which measures the mass change and viscoelasticity variation of materials/virus by measuring the frequency and damping change of a piezoelectric quartz crystal resonator [61,62]. Piezoelectric materials generate electric field/potential under external pressure, and this phenomenon is known as the direct piezoelectric effect. Conversely, when an electric field is applied on the opposite surface of the piezoelectric crystal, the materials undergo mechanical distortion and show expansion and contraction. The converse piezoelectric effect plays a crucial role to design the coronavirus biosensors, where the mass of molecules adsorbed or desorbed from the piezoelectric crystal surface are the origin of the transduction mechanism and graphene interdigitated gold electrode piezoelectric sensor for rapid and specific detection of *Staphylococcus aureus* is also reported [63,64]. To detect the SARS associated coronavirus (SARS-CoV) in sputum, Zuo et al. have successfully demonstrated a piezoelectric immunosensor [65]. In the reported work, a horse polyclonal antibody against SARS-CoV has bounded on the piezoelectric crystal surface in an ordered orientation through protein. They have demonstrated that when the antigen sample was atomized into an aerosol, the antibody on the crystal adsorbed the SARS antigen and the change in the mass of piezoelectric crystal leads to a frequency shift. The schematic of the device configuration is presented in Fig. 5a. It was clearly shown that the frequency shifts have a linear dependency on antigen concentration in the range of 0.6–4 µg/mL [65]. The developed piezoelectric device exhibited good reproducibility and can be reused 100 times without a detectable loss of activity [60].

The schematic representation of the piezoelectric quartz microbalance biosensor along with the computer-controlled signal detector is shown in Fig. 5b. The relation of frequency to mass for piezoelectric quartz crystal resonator is governed by the following equation:

$$\Delta f = - (F^2 \Delta m / N A \rho)$$

where Δf is the change in resonance frequency, F is the resonance frequency of the crystal, ρ is the density of the crystal, Δm is the mass change, n is the overtone number, and A is the area. Moreover, such a piezoelectric biosensor was not able to only detect the coronavirus but was also successfully used to detect the human immunodeficiency virus type 1 (HIV-1). Nicoletta Giamblanco et al. have developed the single step and label-free method to selectively detect the hepatitis B virus (HBV) genome based on hybridization
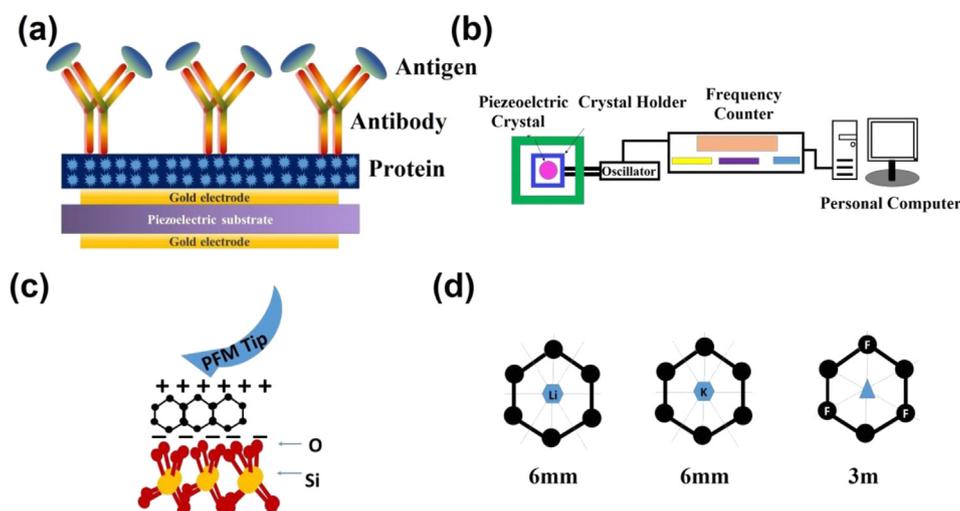
Fig. 5. (a) Schematic of the absorption of coronavirus and (b) experimental set up to record the data. (c) Piezoelectricity in graphene on SiO_2 substrate and (d) piezoelectric property in graphene through Li and F doping.

with simple linear ssDNA probes immobilized on the Au surfaces of a piezoelectric quartz crystal microbalance resonator [66]. They demonstrated the selective sensing of large DNA targets, constituted by an HBV clone of 7 kbps, through optimization of the probe density by piezoelectric sensors. In this work, the immobilization of thiol-labeled ssDNA oligonucleotides on the Au surfaces has been studied *in situ* by piezoelectric quartz crystal microbalance biosensor. They have measured real-time acoustic curves in a concentration range of 0.8−38.8 mM for the two different probes and detectable amounts of adsorbed probes were observed. The working mechanism of the sensor was described by the piezoelectric effect and it is proposed that the ssDNA molecules are anchored to the gold, via thiol group, in a standing-up position. The frequency decrease after the rinsing step is attributed to the adsorption of a water shell around the DNA molecules, enabling the ssDNA molecules to extend farther out into the water. The amount of anchored probe was calculated using the measured value of frequency and dissipation changes in probe adsorption [66].

Based on the above discussion and previously reported work it is worth to point out that the change in the frequency and absorption mass is highly correlated to the piezoelectric biosensor for the detection of SARS-CoV and other viruses such as HIV. The piezoelectric crystals frequency depends on the thickness of the crystal materials and the speed of the shear wave. Moreover, the selectivity of the piezoelectric quartz crystal microbalance biosensor to detect SARS-CoV virus strongly depends on the mass changes on the crystal surface, such as hybridization and/or antigen-antibody reactions on the surface of the piezoelectric microbalance. Recently, various groups reported that the functionalized nanoparticles increase the specificity and sensitivity of piezoelectric biosensors [67,68]. Graphene can be used as a piezoelectric two-dimensional (2D) materials to detect the SARS-CoV virus through a piezoelectric crystal microbalance biosensor. CVD grown graphene exhibits a centrosymmetric crystal structure and has proven as an active nanosheet for electrode applications [69]. Recently, strong piezoelectricity in SLG deposited on SiO_2 grating substrates is demonstrated by Andrei Kholkin and his team [70]. Since the pristine graphene layer(s) do not possess any piezoelectric activity due to its intrinsically centrosymmetric crystal structure, piezoelectricity can be induced by breaking of the inversion symmetry. They have reported a vertical piezo-response in SLG on SiO_2 with a piezoelectric charge coefficient of about 1.4 nm/V, considerably higher than

quartz and lead zirconate titanate single crystals, by piezo-response force microscopy. The piezoelectricity in graphene is attributed to the chemical interaction of carbon atoms with oxygen atoms of the substrate that induces non-zero net dipole moment and polarization. The schematic representation of piezoelectricity in graphene on SiO_2 is shown in Fig. 5c.

Ong et al. also reported the piezoelectric effects in non-piezoelectric graphene through the selective surface adsorption of atoms [71]. They demonstrated that the adsorption of the atoms on the surface of graphene breaks inversion symmetry and may show piezoelectricity, comparable to other 2D and 3D materials. Doping of graphene with F and Li leads to the piezoelectric co-efficients of 0.1 V/Å which is important for piezoelectric crystal biosensors (Fig. 5d). Thus, the generation of piezoelectricity in 2D graphene by various approaches could lead to the development of high-performance graphene-based piezoelectrical biosensors for fast and sensitive detection of various bio-molecules and viruses including SARS-CoV-2 virus. The schematic for possible device structure for graphene-based piezoelectric crystal microbalance for the detection of SARS-CoV-2 and other similar viruses is shown in Fig. 6. The pristine and doped graphene can be used as electrode and quartz crystal in the piezoelectric crystal microbalance, respectively, to enhance the sensitivity of the virus through the increase in the binding of antibody/antigen into the conductive graphene surface and improved changes in the mass of the piezoelectric graphene crystal. Table 2 shows the literature on graphene
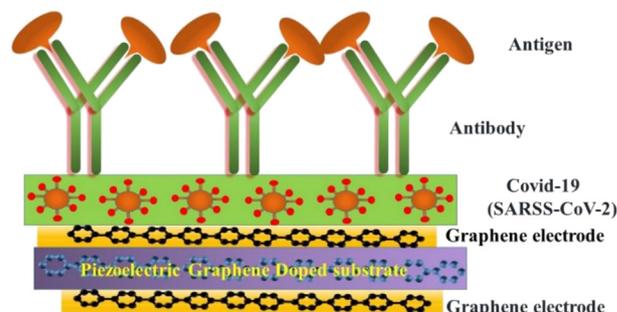

Fig. 6. Schematic of piezoelectric graphene-based absorption of Coronavirus.

and GRMs-based piezoelectric biosensors for the detection of various viruses.

7. Graphene based on gene-editing technology (CRISPR/Cas)

Clustered regularly interspaced short palindromic repeats (CRISPR)-associated nuclease (Cas) proteins, guided by single standard RNA, are emerging potential tools for sequence-specific targeting and detection [80]. Hajian et al. have reported the development of a graphene-based field-effect transistor that uses CRISPR technology, termed as CRISP-Chip, for the label-free digital detection of a target DNA sequence within intact genomic material and termed it as CRISP. In this label-free biosensor device, the graphene is functionalized with a catalytically deactivated Cas9-CRISPR complex (dRNP), which interacts with its target sequence by scanning the complete genomic sample, unzipping the double helix connecting upstream of a protospacer adjacent motif18 until it recognizes and binds to the target DNA sequence that is complementary to the single-guide RNA molecule (sgRNA) within the dRNP. The electrical signal generated by the binding of the targeted DNA sequence by the Cas9-sgRNA complex is recorded via a handheld device without any amplification. The device has a detection time of 15 min with a sensitivity of 1.7 fM [81].

8. 3D printing of graphene/GRMs-composites for medical components

Besides the conventional approach for the component and system developments, 3D printing could also be used for the design and development of graphene/GRMs-based components to be used for COVID-19 [12,67,68]. 3D printing is a powerful and futuristic manufacturing process whereby the properties of the materials can be varied to match the properties of conventional metals and alloy and polymers. GRMs-metal or GRMs-polymer composites have been used to develop components using 3D printing for applications in aerospace structures, engines, electric vehicles, heat exchanger, transformer core, etc. These would result in highly efficient engines, vehicles, and less fuel consumption and less carbon emission. 3D printing has also been used to develop medical components based on GRMs-composites [82]. For example, SS316L- and AlSi10Mg-GRMs composites, both are medical grade materials, were 3D printed, and by varying the amount of GRMs the properties were tuned to suit the need of various spare parts in less lead time [12,83]. The chitosan-graphene, poly(trimethylene carbonate)-graphene, poly(methacrylic acid)-graphene, and poly-ethylene glycol-graphene composites-based scaffolds have been developed employing 3D printing [82]. The current pandemic demonstrates the need for distributed manufacturing of essential items, and hence 3D printing could contribute to the development of several components such as PPEs (face mask, respirators, and face shield) and swabs that are required for virus diagnosis, parts of a ventilator, etc [84]. In particular, due to the appealing properties of graphene and GRMs, the GRMs-metal or GRMs-polymer composites, instead of just metals or polymers, could be used as base materials for 3D printing to achieve better components or systems. Moreover, GRMs display inherent antiviral properties, so the face masks and respirators based on GRMs-polymer composites would not only protect the human from the virus but also contribute to killing the virus. Fig. 7 shows the application of 3D printing in the development of samples/components-based graphene-metal (Fig. 7a) and graphene-polymer composite materials.

9. Multilayer graphene nanofoams

Nanofoams are porous materials, contain nano-sized pores throughout the material, and display many intrinsic and tailorable properties. Thus, nanofoams have huge potential for designing and development of a number of components needed to fight against infectious diseases such as COVID-19. Multilayer graphene nanofoams in particular are important due to their ultra-low density, high surface area, interconnected nanoporous structure, excellent mechanical strength, high electrical and thermal conductivities, high chemical, and corrosion resistant, and antimicrobial and antiviral efficacy [14,85−88]. These nanofoams can be prepared by a number of techniques such as CVD, powder metallurgy templates, freeze-drying, sol-gel, blowing agents, 3D printing, dip-coating on a porous framework, and hydrothermal [89], employing different carbon precursors namely resin, polymers, pitches, coal, graphite, GO, and so on. The controlled porosity on nano-sizes could be an important characteristic of multilayer graphene-based nanofoams to design and develop highly efficient face masks in particular for SARS-CoV-2. The ordered nanoporous carbon materials with a size of less than 100 nm have been synthesized by researchers [90]. Nanoporous carbons with pore sizes in the range of 10−100 nm and extremely high surface areas have been prepared using silica nanoparticles as templates [90]. Similarly, Huang et al. [86] have developed nanoporous graphene foams with the controlled pore size ~ 100 nm using graphene oxide and silica spherical particles as
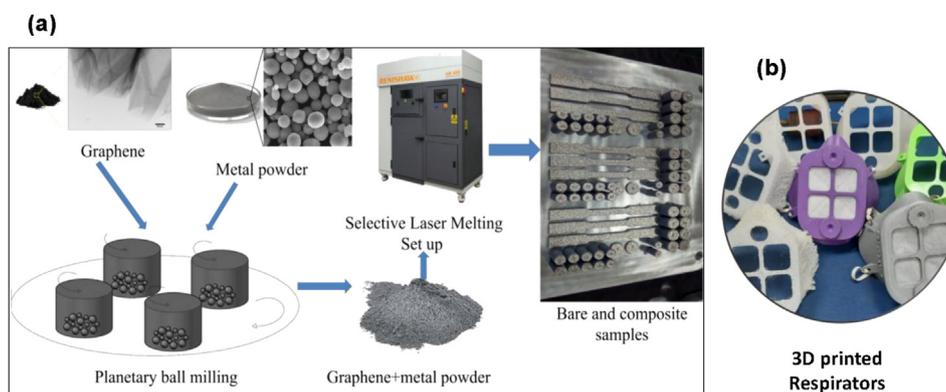

Fig. 7. (a) Graphene reinforced composites were made using a selective laser melting technique, where graphene-coated metal powders were employed to make the components [12,83]. (b) 3D printing was employed to develop polymer-graphene composites-based respirators.
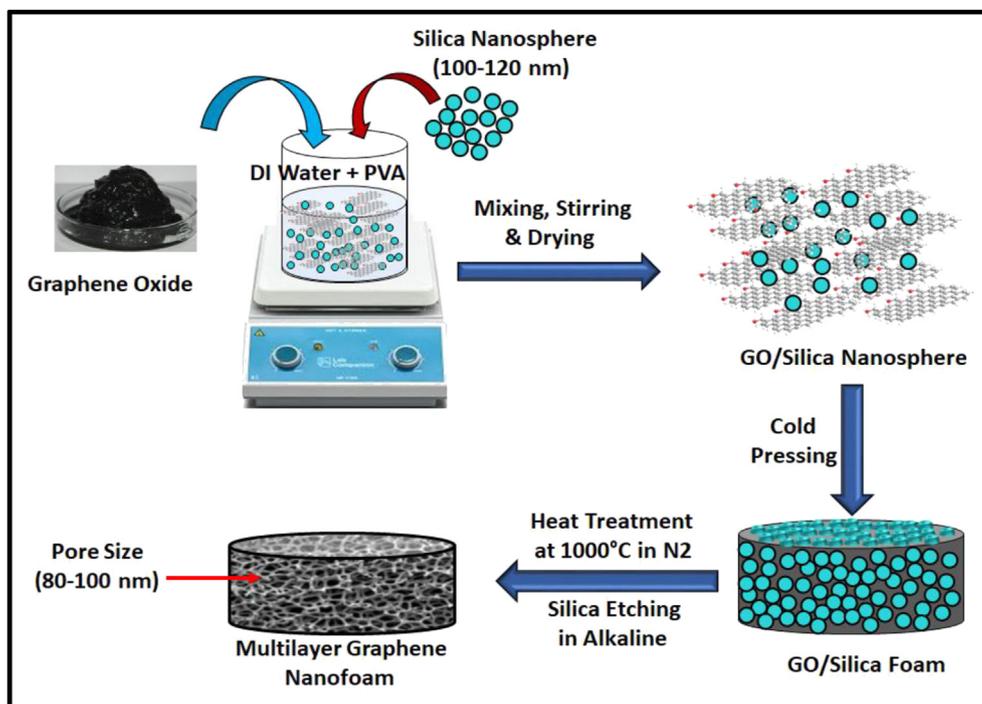
Fig. 8. Schematic representation for the fabrication of multilayer graphene nanofoams.

a template. Presently, the N-95 face mask, a face mask that blocks about 95% of contaminant particles and contains a filter of pore size about 300 nm, is popular among the masks category to protect infection transmission [91]. However, due to a pore size of about 300 nm, there is considerable loss in filtration efficacy of N-95 for sub-300 nm contaminant particles. It is important to note that the size of the SARS-CoV-2 is ~60−140 nm [92]. Sneezing may produce few thousands of droplets of diameter about 500−1200 nm [93]. Likewise, coughing produces droplets of size mainly below 1000 nm [93]. These droplets may contain significant and variable amounts of contaminant particles which could be germs and viruses. However, the liquid in droplets may evaporate and their size could be reduced while traveling in the air for quite sometime [94]. Thus, present N-95 masks though effectively protect the transmission of sneezing or coughing droplets, lower-sized (sub-300 nm) particles may not be completely blocked. Moreover, it is proposed that the SARS-CoV-2 virus may stay in the air for some time [16]. Thus, designing of face mask with a pore size less than 300 nm could be an effective strategy to combat infection problems, in particular against COVID-19. Taking this on a serious note, recently, Al-Etab et al. [95] worked on developing an improved N-95 face mask with a pore size lower than 300 nm. Indeed, they developed a polyimide membrane with pore sizes between 5 and 55 nm using plasma and lithography technologies, and the developed membrane could be used in improved N-95 face masks to effectively block SARS-CoV-2 whose size is higher than the size of nanopores created in polyimide membrane [96]. Multilayer graphene nanofoams-based filters with pore size about 100 nm or lower may also be developed for developing improved N-95 face masks for special purpose uses, though such filters must pass the strict test against air flow rate, pressure change, and other essential parameters required for face masks. Fig. 8 shows a possible strategy to design multilayer graphene nanofoams with pore size about 100 nm which could be scaled down to sub-50 nm by materials

engineering. Thus, multilayer graphene nanofoams have potential for the development of effective healthcare components in particular for the development of efficient face masks.

10. Graphene-based surface plasmon resonance substrate

Gold nanomaterials are commonly used as surface plasmon resonance (SPR) substrate for biomolecule detection and chemical sensing [97]. The signature of chemical moiety gets increased due to the interaction of electromagnetic waves with gold nanoparticles. The molecules, which are '*hard-to-find*,' can be easily detected using the SPR effect of gold nanoparticles. The SPR effect has also been observed with a graphene sheet, a two-dimensional sheet with nanoscale features, where the unpaired 2p electron on the nanographene sheet can enhance the signal of chemical or biomolecules by several folds. Thus, SPR characteristics of graphene-based materials can be exploited for the detection of viruses using a spectroscopic technique such as Raman spectroscopy. Fig. 9 shows the concept of SPR in graphene-based materials. When an electromagnetic (EM) wave strikes the graphene surface the electron cloud of graphene sheets interacts with radiation, leading to enhancement of Raman signal. The schematic for enhancement of signal (red curve) with respect to the original signal (blue curve), as a consequence of the SPR effect, is also shown in Fig. 9. Wu et al. reported the graphene decorated gold film for SPR applications [97]. Theoretically, the relationship between the number of graphene layers and the sensitivity of SPR was shown using the Kretschmann excitation concept. Ten layers of graphene in the film increase SPR sensitivity by twenty-five percent. This increment in SPR sensitivity may be assigned to charge-transfer from graphene to Au nanoparticles in the film. Salihoglu et al. demonstrated the application of graphene-coated gold-silver film for enhancing the SPR sensitivity [98]. Graphene was prepared by a chemical vapor deposition process and then transferred using a
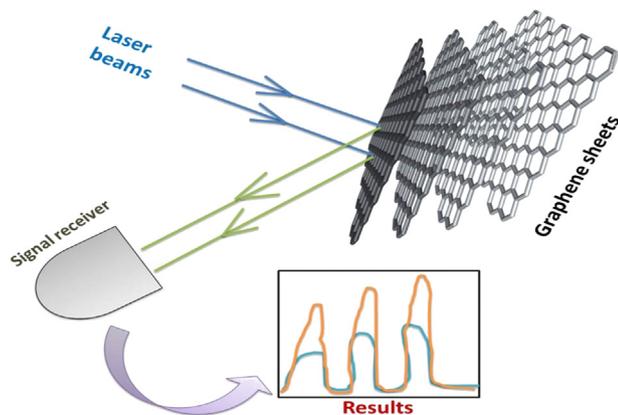
Fig. 9. Schematic for the basic concept of SPR effect on graphene sheets.

PDMS stamp and etched through $FeCl_3$ solution. The serum albumin protein was attached with graphene sheets to check the performance of the composite film. The low value of dissociation constant indicates the strong binding between the graphene sheet and serum albumin protein. Sreekanth et al. investigated the variation in SPR sensitivity by changing the thickness of the gold and the number of graphene layers [99]. The 45-nm thick gold film shows the maximum sensitivity, which is found to be comparable to the sensitivity achieved using only four layers of graphene [99]. Thus, at reduced thicknesses, the performance of graphene-based SPR substrate can outperform the conventional gold substrate. Zhang research group prepared a composite of graphene oxide and gold nanoparticles through well-known Hammers and Offerman methods [100]. Atomic force microscopy was deployed for the quality assessment of graphene oxide and its arrangement with gold nanoparticles. To observe the SPR effect of the gold-graphene oxide composite film, human IgG was taken into the investigation as a target analyte. A wavelength modulation was used in the SPR sensor to observe antibody-antigen binding interactions. The composite film was decorated with goat anti-human IgG as a capture antibody. The target solution having human IgG passed onto the composite film surface to find the detection limit of the system. The detection limit of the gold-graphene oxide film was four times higher than pure gold film alone. Hu et al. functionalized the graphene oxide sheets with polydopamine through oxidative polymerization in an alkaline medium for the detection of biomarkers in serum [101]. An SPR chip was developed by depositing gold over the film to further enhance the sensitivity. The detection limit of 500 pg mL^{-1} was reported with a carcinoembryonic antigen in 10% human serum. These findings reinforce that graphene-based SPR substrates could be used for designing and development of the sensitivity devices for the detection of SARS-CoV-2 and other viruses. In particular, due to synergistic effects, the hybrid graphene/GRMs-Au nanoparticles-based materials could be more promising for designing SPR-based diagnostic systems and devices.

11. Conclusive remark and future prospects

Graphene and GRMs for healthcare applications is one of the fastest-growing fields of science and technology. In particular, graphene and GRMs have shown promise to combat viral diseases via the development of excellent diagnostic devices, and control of infection spread through the development of various components and coatings. In this article, we compiled the literature and discussed the use of graphene and GRMs in antiviral coatings, protective components, and diagnostic devices to combat virus-driven diseases including COVID-19. We discussed in detail various functional properties of graphene, GRMs, and their composites. Specifically, graphene, GRMs, and their composites with metals and polymers could be used for the development of (i) antimicrobial and antiviral coatings to prevent the infection spread from high touch surfaces, (ii) electrochemical, FET, piezoelectric, and CRISPR technology-based biosensors for early, fast and sensitive diagnosis of viruses including SARS-CoV-2, (iii) various PPEs and other healthcare systems based on 3D printing technology, (iv) nanofoams with controlled and smaller pore size for an improved face mask, (v) SPR substrates for sensitive diagnosis of biomolecules and viruses.

While the graphene, GRMs, and their composite have shown excellent functional properties for healthcare applications, the medical components, devices, etc. have not yet advanced to the clinical trial stage. This indicates that the path of graphene and GRMs for healthcare applications is still far ahead. Indeed, one of the most critical subjects of current and future research on graphene and GRMs could be advancing the work up to the clinical trials stage and then product development in terms of commercial diagnostic devices, protective components, surface coatings, etc. Interestingly, even in this present COVID-19 scenario, many graphene-based protective equipment/components have been developed such as face mask, 3D printed components, biosensors, and surface coatings, and some of these technologies are expected to convert into commercial products in near future. Overall, while the path for graphene and GRMs to reach the product level seems to be long, however, recent progress in science and technology of these materials for medical applications may help to achieve the commercialization target soon.

Data availability statement

Data is available upon request.

Funding

Declaration of competing interest

The authors declare that they have no known competing financial interests or personal relationships that could have appeared to influence the work reported in this paper.

References

[1] A.C. Walls, Y.-J. Park, M.A. Tortorici, A. Wall, A.T. McGuire, D. Veesler, Cell 181 (2020) 281–292, e286.
[2] J. Shang, G. Ye, K. Shi, Y. Wan, C. Luo, H. Aihara, Q. Geng, A. Auerbach, F. Li, Nature 581 (2020) 221–224.
[3] https://www.worldometers.info/coronavirus/.
[4] K.S. Novoselov, A. Geim, Nat. Mater. 6 (2007) 183–191.
[5] A.C. Ferrari, F. Bonaccorso, V. Fal'Ko, K.S. Novoselov, S. Roche, P. Bøggild, S. Borini, F.H. Koppens, V. Palermo, N. Pugno, Nanoscale 7 (2015) 4598–4810.
[6] R. Pasricha, S. Gupta, A.K. Srivastava, Small 5 (2009) 2253–2259.
[7] N.O. Weiss, H. Zhou, L. Liao, Y. Liu, S. Jiang, Y. Huang, X. Duan, Adv. Mater. 24 (2012) 5782–5825.

[8] N. Dwivedi, T. Patra, J.-B. Lee, R.J. Yeo, S. Srinivasan, T. Dutta, K. Sasikumar, C. Dhand, S. Tripathy, M.S.M. Saifullah, A. Danner, S.A.R. Hashmi, A.K. Srivastava, J.-H. Ahn, S.K.R.S. Sankaranarayanan, H. Yang, C.S. Bhatia, Nano Lett. 20 (2020) 905−917.

[9] M.D. Mukherjee, C. Dhand, N. Dwivedi, B.P. Singh, G. Sumana, V.V. Agarwal, J.S. Tawale, B.D. Malhotra, Sensor. Actuator. B Chem. 210 (2015) 281−289.

[10] R. Devi, S. Gogoi, H.S. Dutta, M. Bordoloi, S.K. Sanghi, R. Khan, Nanoscale Advances 2 (2020) 239−248.

[11] D.K. Bharti, M.K. Gupta, R. Kumar, N. Sathish, A.K. Srivastava, Nano Energy (2020) 104821.

[12] G.S. Tiwari, A. Mandal, N. Sathish, A. Agrawal, A. Srivastava, Additive Manufacturing 33 (2020) 101095.

[13] H.E. Karahan, C. Wiraja, C. Xu, J. Wei, Y. Wang, L. Wang, F. Liu, Y. Chen, Adv. Healthcare Mater 7 (2018) 1701406.

[14] X. Zou, L. Zhang, Z. Wang, Y. Luo, J. Am. Chem. Soc. 138 (2016) 2064−2077.

[15] V. Palmieri, M. Papi, Nano Today (2020) 100883.

[16] B. Udugama, P. Kadhiresan, H.N. Kozlowski, A. Malekjahani, M. Osborne, V.Y. Li, H. Chen, S. Mubareka, J.B. Gubbay, W.C. Chan, ACS Nano 14 (2020) 3822−3835.

[17] A. Cordaro, G. Neri, M.T. Sciortino, A. Scala, A. Piperno, Nanomaterials 10 (2020) 1014.

[18] X. Li, W. Cai, J. An, S. Kim, J. Nah, D. Yang, R. Piner, A. Velamakanni, I. Jung, E. Tutuc, S.K. Banerjee, L. Colombo, R.S. Ruoff, Science 324 (2009) 1312−1314.

[19] H.-j. Kwon, J.M. Ha, S.H. Yoo, G. Ali, S.O. Cho, Nanoscale Res. Letters 9 (2014) 1−6.

[20] P. Sutter, J.T. Sadowski, E. Sutter, Phys. Rev. B 80 (2009) 245411.

[21] N.A. Vinogradov, A. Zakharov, V. Kocevski, J. Rusz, K. Simonov, O. Eriksson, A. Mikkelsen, E. Lundgren, A. Vinogradov, N. Mårtensson, Phys. Rev. Lett. 109 (2012), 026101.

[22] T. Wu, X. Zhang, Q. Yuan, J. Xue, G. Lu, Z. Liu, H. Wang, H. Wang, F. Ding, Q. Yu, Nat. Mater. 15 (2016) 43−47.

[23] M. Chen, R.C. Haddon, R. Yan, E. Bekyarova, Mater Horizons 4 (2017) 1054−1063.

[24] D.C. Marcano, D.V. Kosynkin, J.M. Berlin, A. Sinitskii, Z. Sun, A. Slesarev, L.B. Alemany, W. Lu, J.M. Tour, ACS Nano 4 (2010) 4806−4814.

[25] P. Tian, L. Tang, K. Teng, S. Lau, Mater. Today. Chem 10 (2018) 221−258.

[26] F. Wu, S. Zhao, B. Yu, Y.-M. Chen, W. Wang, Z.-G. Song, Y. Hu, Z.-W. Tao, J.-H. Tian, Y.-Y. Pei, Nature 579 (2020) 265−269.

[27] V. Stadnytskyi, C.E. Bax, A. Bax, P. Anfinrud, Proc. Natl. Acad. Sci. Unit. States Am. 117 (2020) 11875−11877.

[28] N. Van Doremalen, T. Bushmaker, D.H. Morris, M.G. Holbrook, A. Gamble, B.N. Williamson, A. Tamin, J.L. Harcourt, N.J. Thornburg, S.I. Gerber, N. Engl. J. Med. 382 (2020) 1564−1567.

[29] A. Chin, J. Chu, M. Perera, K. Hui, H.-L. Yen, M. Chan, M. Peiris, L. Poon, medRxiv (2020).

[30] F. Perreault, A.F. De Faria, S. Nejati, M. Elimelech, ACS Nano 9 (2015) 7226−7236.

[31] W. Hu, C. Peng, W. Luo, M. Lv, X. Li, D. Li, Q. Huang, C. Fan, ACS Nano 4 (2010) 4317−4323.

[32] C. Li, X. Wang, F. Chen, C. Zhang, X. Zhi, K. Wang, D. Cui, Biomaterials 34 (2013) 3882−3890.

[33] M. Sametband, I. Kalt, A. Gedanken, R. Sarid, ACS Appl. Mater. Interfaces 6 (2014) 1228−1235.

[34] S. Ye, K. Shao, Z. Li, N. Guo, Y. Zuo, Q. Li, Z. Lu, L. Chen, Q. He, H. Han, ACS Appl. Mater. Interfaces 7 (2015) 21571−21579.

[35] Z. Song, X. Wang, G. Zhu, Q. Nian, H. Zhou, D. Yang, C. Qin, R. Tang, Small 11 (2015) 1171−1176.

[36] Y.-N. Chen, Y.-H. Hsueh, C.-T. Hsieh, D.-Y. Tzou, P.-L. Chang, Int. J. Environ. Res. Publ. Health 13 (2016) 430.

[37] X.X. Yang, C.M. Li, Y.F. Li, J. Wang, C.Z. Huang, Nanoscale 9 (2017) 16086−16092.

[38] T. Du, J. Lu, L. Liu, N. Dong, L. Fang, S. Xiao, H. Han, ACS Applied Bio Mater. 1 (2018) 1286−1293.

[39] P.B.v. Kasteren, B.v.d. Veer, S.v.d. Brink, L. Wijsman, J.d. Jonge, A.v.d. Brandt, R. Molenkamp, C.B. Reusken, A. Meijer, J. Clin. Virol. 128 (2020) 104412.

[40] M. Pividori, A. Merkoci, S. Alegret, Biosens. Bioelectron. 15 (2000) 291−303.

[41] F. Lucarelli, G. Marrazza, A.P. Turner, M. Mascini, Biosens. Bioelectron. 19 (2004) 515−530.

[42] D. Nidzworski, K. Siuzdak, P. Niedziałkowski, R. Bogdanowicz, M. Sobaszek, J. Ryl, P. Weiher, M. Sawczak, E. Wnuk, W.A. Goddard, Sci. Rep. 7 (2017) 1−10.

[43] L.A. Layqah, S. Eissa, Microchimica Acta 186 (2019) 224.

[44] E. Bakker, Anal. Chem. 76 (2004) 3285−3298.

[45] S. Islam, S. Shukla, V.K. Bajpai, Y.-K. Han, Y.S. Huh, A. Kumar, A. Ghosh, S. Gandhi, Biosens. Bioelectron. 126 (2019) 792−799.

[46] M. Pumera, Mater. Today 14 (2011) 308−315.

[47] J. Peña-Bahamonde, H.N. Nguyen, S.K. Fanourakis, D.F. Rodrigues, J. Nanobiotechnol. 16 (2018) 75.

[48] S. Afsahi, M.B. Lerner, J.M. Goldstein, J. Lee, X. Tang, D.A. Bagarozzi Jr., D. Pan, L. Locascio, A. Walker, F. Barron, Biosens. Bioelectron. 100 (2018) 85−88.

[49] S.R. Joshi, A. Sharma, G.-H. Kim, J. Jang, Mater. Sci. Eng. C 108 (2020) 110465.

[50] J. Huang, Z. Xie, Z. Xie, S. Luo, L. Xie, L. Huang, Q. Fan, Y. Zhang, S. Wang, T. Zeng, Anal. Chim. Acta 913 (2016) 121−127.

[51] A. Srivastava, N. Dwivedi, C. Dhand, R. Khan, N. Sathish, Science Reporter 57 (2020) 32−35.

[52] Y. Chen, R. Ren, H. Pu, X. Guo, J. Chang, G. Zhou, S. Mao, M. Kron, J. Chen, Sci. Rep. 7 (2017) 1−8.

[53] T. Ono, T. Kawata, Y. Kanai, Y. Ohno, K. Maehashi, K. Inoue, Y. Watanabe, S. Nakakita, Y. Suzuki, T. Kawahara, 2018 76th Device Research Conference (DRC), IEEE, 2018, pp. 1−2.

[54] J.W. Kim, S. Kim, Y.-h. Jang, K.-i. Lim, W.H. Lee, Nanotechnology 30 (2019) 345502.

[55] X. Jin, H. Zhang, Y.-T. Li, M.-M. Xiao, Z.-L. Zhang, D.-W. Pang, G. Wong, Z.-Y. Zhang, G.-J. Zhang, Microchimica Acta 186 (2019) 223.

[56] M. Pant, H. Kharkwal, K. Singh, H. Joshi, Biosens. J. 6 (2017) 2.

[57] G. Seo, G. Lee, M.J. Kim, S.-H. Baek, M. Choi, K.B. Ku, C.-S. Lee, S. Jun, D. Park, H.G. Kim, ACS Nano 14 (2020) 5135−5142.

[58] A. Shons, F. Dorman, J. Najarian, J. Biomed. Mater. Res. 6 (1972) 565−570.

[59] N.M. do Nascimento, A. Juste-Dolz, E. Grau-García, J.A. Román-Ivorra, R. Puchades, A. Maquieira, S. Morais, D. Gimenez-Romero, Biosens. Bioelectron. 90 (2017) 166−173.

[60] M. Pohanka, Talanta 178 (2018) 970−973.

[61] F.N. Meyers, K.J. Loh, J.S. Dodds, A. Baltazar, Nanotechnology 24 (2013) 185501.

[62] G. Sauerbrey, Zeitschrift für physik 155 (1959) 206−222.

[63] A.L. Olsson, I.R. Quevedo, D. He, M. Basnet, N. Tufenkji, ACS Nano 7 (2013) 7833−7843.

[64] X. Huang, J. Xu, H.-F. Ji, G. Li, H. Chen, Analytical Methods 6 (2014) 4530−4536.

[65] B. Zuo, S. Li, Z. Guo, J. Zhang, C. Chen, Anal. Chem. 76 (2004) 3536−3540.

[66] N. Giamblanco, S. Conoci, D. Russo, G. Marletta, RSC Adv. 5 (2015) 38152−38158.

[67] M. Pohanka, Materials 11 (2018) 448.

[68] X. Guo, C.-S. Lin, S.-H. Chen, R. Ye, V.C. Wu, Biosens. Bioelectron. 38 (2012) 177−183.

[69] S. Kim, M.K. Gupta, K.Y. Lee, A. Sohn, T.Y. Kim, K.-S. Shin, D. Kim, S.K. Kim, K.H. Lee, H.-J. Shin, D.-W. Kim, S.-W. Kim, Adv. Mater. 26 (2014) 3918−3925.

[70] G. da Cunha Rodrigues, P. Zelenovskiy, K. Romanyuk, S. Luchkin, Y. Kopelevich, A. Kholkin, Nat. Commun. 6 (2015) 1−6.

[71] M.T. Ong, E.J. Reed, ACS Nano 6 (2012) 1387−1394.

[72] Ü. Anik, Y. Tepeli, M. Sayhi, J. Nsiri, M.F. Diouani, Analyst 143 (2018) 150−156.

[73] R. Singh, S. Hong, J. Jang, Sci. Rep. 7 (2017) 42771.

[74] S.-A. Jin, S. Poudyal, E.E. Marinero, R.J. Kuhn, L.A. Stanciu, Electrochim. Acta 194 (2016) 422−430.

[75] A. Valipour, M. Roushani, Biosens. Bioelectron. 89 (2017) 946−951.

[76] A. Nehra, W. Chen, D.S. Dimitrov, A. Puri, K.P. Singh, ACS Appl. Mater. Interfaces 9 (2017) 32621−32634.

[77] S. Mahari, A. Roberts, D. Shahdeo, S. Gandhi, bioRxiv (2020).

[78] Y. Lian, F. He, H. Wang, F. Tong, Biosens. Bioelectron. 65 (2015) 314−319.

[79] S.-H. Chen, Y.-C. Chuang, Y.-C. Lu, H.-C. Lin, Y.-L. Yang, C.-S. Lin, Nanotechnology 20 (2009) 215501.

[80] J.S. Gootenberg, O.O. Abudayyeh, J.W. Lee, P. Essletzbichler, A.J. Dy, J. Joung, V. Verdine, N. Donghia, N.M. Daringer, C.A. Freije, Science 356 (2017) 438−442.

[81] R. Hajian, S. Balderston, T. Tran, T. DeBoer, J. Etienne, M. Sandhu, N.A. Wauford, J.-Y. Chung, J. Nokes, M. Athaiya, Nature Biomed Engineering 3 (2019) 427−437.

[82] S. Sayyar, D.L. Officer, G.G. Wallace, J. Mater. Chem. B 5 (2017) 3462−3482.

[83] A. Mandal, J.K. Tiwari, N. Sathish, A.K. Srivastava, Mater. Sci. Eng., A 774 (2020) 138936.

[84] https://www.3dsystems.com/.

[85] Z. Chen, W. Ren, L. Gao, B. Liu, S. Pei, H.-M. Cheng, Nat. Mater. 10 (2011) 424−428.

[86] X. Huang, K. Qian, J. Yang, J. Zhang, L. Li, C. Yu, D. Zhao, Adv. Mater. 24 (2012) 4419−4423.

[87] X. Liu, D. Chao, Y. Li, J. Hao, X. Liu, J. Zhao, J. Lin, H.J. Fan, Z.X. Shen, Nano Energy 17 (2015) 43−51.

[88] Y. Wang, H. Li, J. Kong, Sensor. Actuator. B Chem. 193 (2014) 708−714.

[89] A. Idowu, B. Boesl, A. Agarwal, Carbon 135 (2018) 52−71.

[90] J. Lee, S. Han, T. Hyeon, J. Mater. Chem. 14 (2004) 478−486.

[91] V. Wiwanitkit, Lung 184 (2006) 373.

[92] N. Zhu, D. Zhang, W. Wang, X. Li, B. Yang, J. Song, X. Zhao, B. Huang, W. Shi, R. Lu, N. Engl. J. Med. 382 (2020) 727−733.

[93] P. Bahl, C. Doolan, C. de Silva, A.A. Chughtai, L. Bourouiba, C.R. MacIntyre, J. Infect. Dis. (2020) 1−8, https://doi.org/10.1093/infdis/jiaa189.

[94] H. Holterman, Kinetics and Evaporation of Water Drops in Air, Citeseer, 2003.

[95] N. El-Atab, N. Qaiser, H.S. Badghaish, S.F. Shaikh, M.M. Hussain, ACS Nano 14 (2020) 7659.

[96] S. Zeng, D. Baillargeat, H.-P. Ho, K.-T. Yong, Chem. Soc. Rev. 43 (2014) 3426−3452.

[97] L. Wu, H. Chu, W. Koh, E. Li, Optic Express 18 (2010) 14395−14400.

[98] O. Salihoglu, S. Balci, C. Kocabas, Appl. Phys. Lett. 100 (2012) 213110.

[99] K.V. Sreekanth, S. Zeng, K.-T. Yong, T. Yu, Sensor. Actuator. B Chem. 182 (2013) 424–428.
[100] H. Zhang, Y. Sun, S. Gao, J. Zhang, H. Zhang, D. Song, Small 9 (2013) 2537–2540.
[101] W. Hu, G. He, H. Zhang, X. Wu, J. Li, Z. Zhao, Y. Qiao, Z. Lu, Y. Liu, C.M. Li, Anal. Chem. 86 (2014) 4488–4493.

Dr. N. Sathish is a Principal Scientist at CSIR-Advanced Materials and Processes Research Institute, Bhopal, India. His current research interest includes 3D printing, composite materials and graphene-based materials for multiple applications.

Dr. A. K. Srivastava is presently the Director of CSIR-Advanced Materials and Processes Research Institute, Bhopal, India. His research interest includes characterization of nanomaterials using electron microscopy, and exploration of nanomaterials, graphene-based materials, and metal oxides for wide-spectrum applications.

Dr. Manoj K. Gupta is a Scientist at CSIR-Advanced Materials and Processes Research Institute, Bhopal, India. His current research interest includes graphene-based materials, piezoelectric materials, piezoelectric nanogenerators, and sensors.

Dr. Neeraj Dwivedi is a Principal Scientist at CSIR-Advanced Materials and Processes Research Institute, Bhopal, India. His research interest includes interface engineering, carbon nanocoatings, 2D materials such as graphene-based materials, metal oxides and nitrides for tribological, energy, sensing and antimicrobial applications.

Dr. Rajeev Kumar is an INSPIRE Faculty at CSIR-Advanced Materials and Processes Research Institute, Bhopal, India. His current research interest includes graphene-based porous materials, EMI shielding, micro and nanofoams-based technologies.

Dr. Chetna Dhand is a Senior Scientist at CSIR-Advanced Materials and Processes Research Institute, Bhopal, India. Her research interest includes nanocoatings, nanomaterials, biomaterials, graphene based materials for biosensors, food packaging and antimicrobial applications.

Dr. Raju Khan is a Princiapal Scientist at CSIR-Advanced Materials and Processes Research Institute, Bhopal, India. His current research interest includes bio-molecular separation, nanostructured material-based electrochemical & fluorescence biosensor devices for detection of cancer, cardiovascular and neurotransmitter diseases.

Dr. Surender Kumar is a Scientist at CSIR-Advanced Materials and Processes Research Institute, Bhopal, India. His current research interest includes graphene-based materials, energy storage devices, SPR-based technologies.